

See discussions, stats, and author profiles for this publication at: <https://www.researchgate.net/publication/272137160>

CO₂ Gasification Rates of Petroleum Coke in a Pressurized Flat-Flame Burner Entrained-Flow Reactor

ARTICLE in ENERGY & FUELS · JULY 2014

Impact Factor: 2.79 · DOI: 10.1021/ef500690j

CITATIONS

3

READS

23

3 AUTHORS, INCLUDING:



Thomas H. Fletcher

Brigham Young University - Provo Main Campus

155 PUBLICATIONS 2,299 CITATIONS

[SEE PROFILE](#)

CO₂ Gasification Rates of Petroleum Coke in a Pressurized Flat-Flame Burner Entrained-Flow Reactor

Aaron D. Lewis, Emmett G. Fletcher, and Thomas H. Fletcher*

Department of Chemical Engineering, Brigham Young University, Provo, Utah 84602, United States

ABSTRACT: Two petcoke samples were gasified by CO₂ at total pressures of 10 and 15 atm in a high-pressure flat-flame burner reactor at conditions where the bulk phase consisted of either 40 or 90 mol % CO₂ with gas temperatures up to 1909 K. Particle diameters of 45–75 μm were used in the experiments. The morphology of the two petroleum coke chars was drastically different and evaluated using scanning electron microscopy images of the chars. The mass release data caused by CO₂ gasification of the petcoke chars were fit to a global first-order model, and the optimal kinetic parameters are reported. The CO₂ char gasification rates of both petcoke were shown to be higher than Illinois #6 coal when reacted at conditions of high temperature and pressure, even though most reactivity comparisons between petcoke and coal at lower temperature, pressure, and heating rates typically result in coal being more reactive.

1. INTRODUCTION

Petroleum coke is a byproduct from oil refining that consists primarily of carbon, resembles coal in appearance, and is often referred to as “petcoke”. This low-volatile solid (i.e., petcoke) results from the Coker process, where heavy residual fuel oil is heated until it cracks into more valuable light compounds that are eventually incorporated into jet fuel, diesel, and other components.¹ Current estimates of worldwide petroleum coke generation as of 2012 were 100 million metric tons per year,² and petcoke production is expected to increase as coker units are added to oil refineries to process cheaper and heavier crudes.

One way that petroleum coke can be transformed into useful products such as energy and chemicals is through gasification, which converts any hydrocarbon through partial oxidation into a gaseous fuel mixture termed synthesis gas (or “syngas”) that is primarily composed of H₂ and CO (the desired products), as well as some CO₂ and H₂O. Although coal is the leading gasifier feedstock in commercial gasification, a significant amount of petcoke is also gasified each year. According to the National Energy Technology Laboratory’s (NETL) Gasification Worldwide Database,³ the projected worldwide syngas capacity in 2016 for coal and petcoke is 75 500 and 12 900 MW_{th}, respectively.

Many CO₂ gasification rates of petcoke have been measured and reported in the literature. For example, Tyler and Smith⁴ measured CO₂ gasification rates for three sizes (220, 900, and 2900 μm) of petcoke in the temperature range 1018–1178 K using CO₂ partial pressures between 0.26 and 1.17 atm. Zamalloa et al.⁵ gasified 105–149 μm diameter petcoke particles isothermally using undiluted CO₂ at temperatures in the range 1173–1573 K at atmospheric pressure after heating the sample at 20 K/min. Zou et al.⁶ heated 85–125 μm petcoke at 25 K/min and then reacted the sample isothermally with CO₂ at 0.99 atm in the temperature range 1248–1323 K. Gu et al.⁷ gasified petcoke isothermally at atmospheric pressure in the temperature range 1223–1673 K after heating the ≤73 μm diameter sample at 30 K/min to the gasification temperature. Wu et al.⁸ performed CO₂ gasification reactivity comparisons

isothermally at 1223 K at atmospheric pressure on petcoke char samples that had been pyrolyzed at different temperatures (1223–1673 K) and total pressures (9.9–29.6 atm). Malekshahian and Hill⁹ gasified isothermally <90 μm diameter petcoke particles with CO₂ that had been heated at 25 K/min in the temperature and pressure range 1173–1248 K and 0.99–23.7 atm, respectively. Although these aforementioned petcoke gasification studies progress the knowledge of the field by mainly reporting gasification rates measured in thermogravimetric analysis (TGA) reactors using chars prepared at atmospheric pressure and low initial particle heating rates, there is much to be learned about petcoke gasification rates at conditions characteristic of commercial entrained-flow gasifiers.

In the current work, CO₂ gasification rates of two industrial samples are reported for petcoke chars generated following in situ pyrolysis at elevated pressure, high temperature, and rapid initial heating rate even though only a few research groups study char gasification rates at these experimentally challenging conditions. Because the chars in this study were generated and reacted at similar conditions as in commercial entrained-flow gasifiers, the measured rates are especially meaningful. For instance, the petcoke chars for which rates are reported in this study would presumably contain a similar char structure as char generated in industrial entrained-flow gasifiers, thus capturing the effect of representative char structure on the burnout of residual char.¹⁰ The present paper also gives a rate comparison between petcoke and coal char at pressurized entrained-flow conditions.

Although it can be implied that petcoke gasification occurs quickly in entrained-flow gasifiers where the maximum residence time is on the order of seconds, the reported petcoke gasification rates in the current literature^{4–9} are on the order of minutes and even hours (at lower temperatures, pressures, and heating rates). The current study reports CO₂ gasification rates

Received: March 27, 2014

Revised: June 4, 2014

Published: June 5, 2014



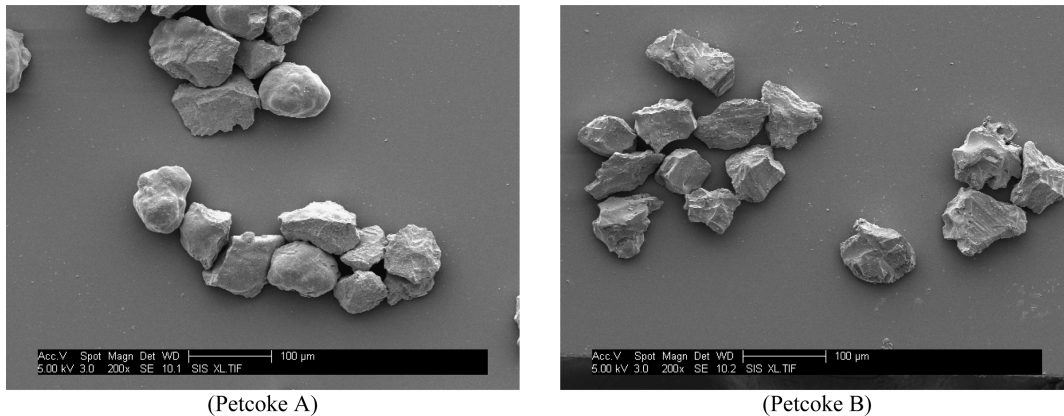


Figure 1. SEM images of raw petcoke samples collected from the 45–75 μm sieve tray.

Table 1. Properties of Feed Stocks

feedstock	Petcoke A	Petcoke B	ILL #6 coal	ILL #6 char	composition of ash (wt %)	
					Petcoke A	Petcoke B
sieved particle size (μm)	45–75	45–75	45–75	75–106	Na	1.0
mass mean size (μm)	63.0	57.6	64.3	85.3	Mg	0.1
C (wt % daf)	87.93	91.09	75.08		Al	0.9
H (wt % daf)	1.82	3.77	5.21		Si	3.9
N (wt % daf)	1.77	1.33	1.34		S	0.4
S (wt % daf)	6.32	2.88	4.35		K	0.7
O (wt % daf, by diff.)	2.16	0.93	14.02		Ca	2.2
volatiles (wt % daf) ^a	8.78	10.52	44.46		Ti	0.3
ash (wt % dry) ^a	0.35	0.30	6.98	13.41	V	37.6
moisture (wt % as rec'd) ^a	1.29	0.20	3.45	2.4	Fe	9.1
apparent density (g/cm^3)	1.58	1.21	1.15	0.16	Ni	9.8
					Cr	1.8
N_2 surface area (m^2/g)	7.5	0.3	44.6	189	Zn	2.2
CO_2 surface area (m^2/g)	187	107	128	343	P	0.9

^aASTM analysis.

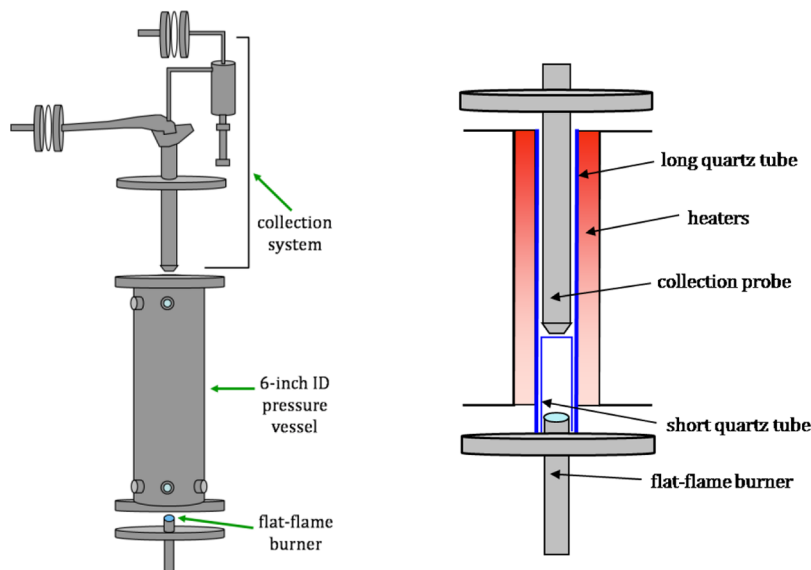


Figure 2. External and cutaway views of BYU's HPFFB reactor.

of two petcoke chars where significant conversions were measured in <300 ms when 45–75 μm diameter particles reacted in an entrained-flow reactor at total pressures of 10 and 15 atm with gas temperatures up to 1909 K. An improved

understanding of the high temperature and pressure gasification reactivity will facilitate better gasifier designs for chemical production or for the integrated gasification combined cycle (IGCC), to generate power.¹¹

Table 2. Matrix of Experiments for Petcoke CO₂ Gasification Tests

total pressure (atm)	max centerline gas temperature (K)	equilibrium CO ₂ , CO, N ₂ , H ₂ O (mol %)	pyrolysis/reference residence time (ms)	petcoke sample	gasification residence times (ms)
15	1848	89.8, 8.1, 1.2, 0.9	59	A	142; 265
			60	B	146; 275
10	1808	89.2, 8.4, 1.2, 1.2	73	A	130; 244
			57	B	137; 258
15	1891	40.8, 11.3, 46.6, 0.7	56	A	137; 259
			60	B	124; 231
10	1909	40.7, 11.0, 46.8, 0.9	52	A	125; 232
			57	B	119; 219

2. EXPERIMENTAL PROCEDURE

Samples. Two commercially obtained petroleum coke samples were studied in this research. The origin and crude oil feedstock from which the petcoke samples originated are proprietary to the companies that supplied the petcoke. The samples are referred to as “Petcoke A” and “Petcoke B” in this paper. Petcoke A has been used in previous research.¹² The petcoke samples were ground using an electric grinder (Blendtec Kitchen Mill) and sieved to collect the 45–75 μm size range, which was used in all the experiments. The small particles were used to ensure a high initial heating rate of the particles, to assume no temperature gradients within the particle for modeling, and to represent the pulverized particle size used in industrial entrained-flow gasifiers. Figure 1 shows scanning electron microscopy (SEM) images of the sized petcoke samples. These pictures, along with other SEM images in this work, were taken using a FEI XL30 ESEM instrument with a field emission gun (FEG) emitter. Properties of the feedstocks used in this study are included in Table 1. Information regarding Illinois #6 coal and its char are included in this table because coal was used in a limited number of experiments reported here.

Note that the ash composition values in Table 1 do not sum to 100, because the elements existed as oxides (i.e., Na₂O, MgO, Al₂O₃, SiO₂, SO₃, K₂O, etc.) after they were collected following an ash test at 750 °C in air. The balance of the ash composition is therefore composed of elemental oxygen. The parent crude oil from which the petcoke samples originated determined the chemical composition of the ash.

Apparatus and Operation. A high-pressure flat-flame burner (HPFFB) reactor was used in this study to measure CO₂ gasification rates of the petroleum coke samples at entrained-flow conditions. A schematic of the reactor is shown in Figure 2. The HPFFB can be used to mimic the reaction environment of industrial entrained-flow reactors. The HPFFB allows small particles that have undergone rapid initial heating rates to react in cocurrent flow at high temperatures and pressures for short times (<1 s).

The flat-flame burner of the HPFFB reactor is roughly 25 mm in diameter and uses about 100 small-diameter tubes to create many diffusion flamelets by feeding gaseous fuel through the tubes while introducing oxidizer in-between the tubes. The numerous small flamelets create a flat flame a few millimeters thick above the burner. Particles were entrained in nitrogen and carried to the middle of the burner surface through a small metal tube (1.346 mm ID). The particles then reacted while traveling upward in laminar flow through a circular quartz tube for known residence times before the particles were quickly quenched with nitrogen in a water-cooled collection probe. A virtual impactor and cyclone in the collection system separated the char aerodynamically while any soot/tar collected on water-cooled filters. Permanent gases traveled through the filters and were released in a ventilation cabinet. Additional details concerning the HPFFB reactor have been reported elsewhere.^{12–16}

Gas temperature was controlled in the HPFFB by adjusting gas flow rates to the burner and the stoichiometry. The experimental matrix of petcoke tests conducted is shown in Table 2 along with the corresponding composition of the postflame environments. The

HPFFB centerline gas temperature profiles were measured using a 422 μm diameter B-type thermocouple¹⁶ corrected for radiation losses. Particle residence time was controlled by adjusting the height between burner and collection probe, and was calculated using particle velocity measurements from a high-speed camera.¹⁶ The four fuel-rich gas conditions used in this study were at total pressures of 10 and 15 atm using postflame CO₂ concentrations near 40 and 90 mol %. Complete details of the petcoke experimental conditions are reported elsewhere.¹⁶

Particles were collected at three residence times per gas condition at typical collection heights of 25, 76, and 140 mm above the burner. The first collection height that was near 25 mm served as a reference data point, because only the mass loss measured after this first collection point was used for modeling purposes. The residence time of this first sample location is included as the “reference residence time” in Table 2. The four gas conditions in this paper (see Table 2) are identified by total pressure, the maximum measured centerline gas temperature, and the mole percentage of CO₂ in the postflame environment.

Mass Release and Replicates. Mass release refers to how much of the initial mass leaves the particle and is an indicator of the extent of gasification when reported on a char basis. Measured mass release after the first collection height was attributed solely to CO₂ gasification of the char; any mass loss from steam gasification was assumed to be negligible due to its low partial pressure (i.e., ~0.12 atm) in the experiments. Although it is possible to calculate mass release using ash as a tracer, this method was not utilized in this study because ash vaporized from petcoke in a previous study¹² when Petcoke A was fed in the HPFFB reactor. The ash-tracer method of calculating mass release only yields correct values when ash truly acts as a tracer and does not leave the particle.

Mass release values used in the gasification modeling of this study were calculated from a mass balance. The best possible mass balance was ensured by shutting down between runs in order to clean out the collection system, and weighing the amount of petcoke fed as well as the collected char. The use of a quartz tube immediately around the burner that extended all the way to the collection probe enabled good collection efficiency (see Figure 2). The collection height of a particular experiment determined the utilized length of this short quartz tube.

The ability to obtain good mass balance data in the HPFFB reactor was evaluated by feeding Petcoke A at a gas condition in the HPFFB where the CO₂ partial pressure and temperature were not sufficiently high to gasify the petcoke char. This condition was at a total pressure of 5 atm in about 20 mol % CO₂ that had a peak gas temperature of 1804 K about 25 mm above the burner. Collection heights in the range 76–241 mm (with corresponding particle residence times 161–620 ms) were used. The average collection efficiency of the HPFFB from five tests was measured to be 98.0%.

Each petcoke mass release data point used in modeling was the average mass release from typically 2 to 3 experiments. The average standard deviations in mass release values at replicate conditions for Petcoke A and B experiments were 3.4 and 3.8 wt % daf, respectively.

3. RESULTS AND DISCUSSION

Pyrolysis Volatile Yields of Petcoke at High Heating Rate.

Both Petcoke A and B were fed through a flat-flame burner reactor in order to test the effect of particle heating rate on the pyrolysis volatiles yield of petroleum coke. A high initial particle heating rate has been shown to increase the volatiles yield during pyrolysis for other solid fuels such as biomass and coal.^{17–20} For example, Borrego et al.¹⁸ measured up to 13% greater volatile yields (or 11 wt % daf) than the daf ASTM volatile yield when pyrolyzing wood chips, forest residues, and rice husks at high heating rate in a drop tube furnace.

Both Petcoke A and B were fed through a flat-flame burner reactor that has been documented previously^{21–24} and operated in a very similar manner as the HPFFB reactor, with the exception of operating at atmospheric pressure. Petcoke A and B were fed at different gas conditions where the peak gas temperature ranged from 1320 to 1929 K in the flat-flame burner reactor using particle residence times in the range 33–102 ms. These experiments served as petcoke pyrolysis experiments at high initial particle heating rate (up to 8.60×10^4 K/s) because no significant mass loss due to CO₂ gasification was measured at these conditions were the bulk CO₂ partial pressure was near 0.21 atm. The average volatiles yield from high heating-rate pyrolysis experiments when feeding Petcoke A was 8.86 wt % (daf), whereas the average mass release of Petcoke B was 10.57 wt % (daf). The results of volatiles yields of Petcoke A and B at both low and high heating-rate conditions are summarized in Table 3. The ASTM

Table 3. Summary of Mass Release from Petcoke Pyrolysis at Low and High Heating Rates at Atmospheric Pressure

sample	ASTM volatiles wt % (daf)	high heating rate volatiles wt % (daf)
Petcoke A	8.78	8.86
Petcoke B	10.52	10.57

volatiles value was taken from Table 1 and serves as a low heating-rate pyrolysis value, whereas the high heating-rate pyrolysis value was taken as the measured mass release during flat-flame burner experiments. There is less than 0.9% difference between the low and high heating-rate pyrolysis mass release values for both petcoke samples. This information is valuable because the char fraction that results from pyrolysis acts as a source of reactants for the thermochemical processes that convert the char, either by combustion or gasification. It is important to note that the comparison in Table 3 was for the effect of heating rate on petcoke volatile yields at atmospheric pressure because increased pressure can result in decreased volatile yields.

Kocaefe et al.²⁵ pyrolyzed four kinds of petroleum coke with ASTM volatile yields ranging from 7.2 to 12.0 wt % in a TGA under N₂ at a relatively low heating rate of 2.43 K/s. It was observed that the ASTM volatiles yield was a good approximation of the volatiles that escaped during pyrolysis in the TGA for each of the four varieties of petcoke. From these TGA experiments in the literature as well as the experiments performed at BYU in a flat-flame burner reactor, the ASTM volatiles yield of petroleum coke appear to be a good estimate for the volatiles yields during both low and high heating-rate conditions at atmospheric pressure.

Morphology of Petcoke Char and Tar Formation. Figure 3 shows partially gasified Petcoke A char that was

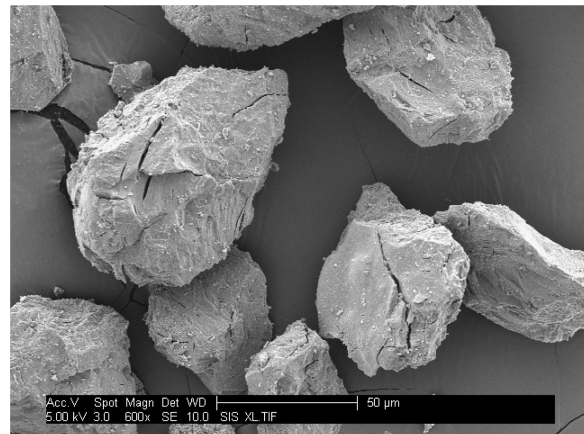


Figure 3. SEM image of partially gasified Petcoke A char collected from the HPFFB reactor.

collected from the HPFFB reactor and serves as a representative image of other collected samples of Petcoke A char. Recall that SEM images of the raw petcoke samples were included in Figure 1. The morphology of Petcoke A char was very similar to that of its parent feedstock material, with the only difference being that the char contains cracks in its surface. Other researchers have also observed cracks and fissures in petcoke char.²⁶ Although less than 9 wt % (daf) volatiles were evolved during pyrolysis of Petcoke A, it is thought that the cracks are likely a result of volatiles escaping the particle interior quickly, which is influenced by the high initial particle heating rates characteristic of flat-flame burner reactors. It should be noted that the cracks observed in Petcoke A char were not substantial enough to cause particle fracturing, which can significantly impact gasification rates. However, the cracks that formed in the petcoke char do create additional surface area that is easily accessible for the reactant gas.

Figure 4 shows partially gasified Petcoke B char, which serves as a representative image of other Petcoke B char collected samples. Petcoke B char collected from the HPFFB contained a mixture of two types of particles. Type 1 char particles closely resembled the parent feedstock particles. Type 2 char particles appeared to be highly swollen cenospheres, similar to Group I coal char that is classified by high porosity, thin walls, and large internal voids.^{27,28} Although reactivity differences between Type 1 and Type 2 petcoke particles have not been reported, to the knowledge of the authors, Group I coal char was cited as being more reactive than dense Group III coal char.¹⁰ Figure 4b provides some insight on the internal structure of the Type 2 char particles. It appears that the swollen char particles from Petcoke B have thin walls with little to no pore network internally. Note that broken and fragmented char particles from Petcoke B, as seen in Figure 4b, were rarely observed in SEM images of the char. Although some cracks were observed in the Type 1 particles of Petcoke B char, the cracks were not nearly as common as was observed in the Petcoke A char particles. It is also noteworthy that other researchers noticed a fraction of cenospheric petcoke char particles following combustion experiments conducted at high heating rate in a drop tube furnace.²⁹

The explanation for cenospheric char particles from softening coals is that the metaplast becomes fluid during devolatilization, which results in an entirely new pore structure.³⁰ Perhaps this explanation for the differences in coal char morphology can also

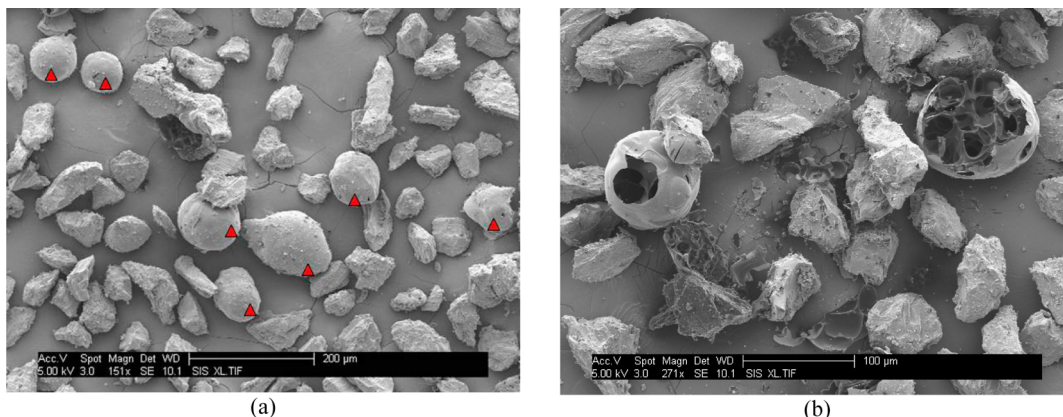


Figure 4. SEM images of partially gasified Petcoke B char collected from the HPFFB reactor. The symbol “▲” identifies Type 2 char particles in panel a.

be applied to Petcoke B. It is interesting to note that although bituminous coals pyrolyzed at high heating rate result in nearly all cenospheric char, the majority of Petcoke B char particles are not cenospheres and did not pass through a plastic stage. Because it is assumed that the differences between the two types of Petcoke B char were caused by transformations during the initial heating of the particle, it would also be assumed that no Type 1 to Type 2 transformation took place during gasification. The different morphologies observed between the chars of Petcoke A and B are possibly attributed to differences in the crude oil feedstock from which the samples originated and perhaps reaction conditions during the coking process, although the exact explanation requires further research.

Although Petcoke B char contained two distinct types of particles, Type 1 particles likely comprised most of the sample mass after pyrolysis due to the very low density of cenospheric char particles. For example, cenospheric bituminous coal char particles had apparent densities 2–11 times less than their parent coal feedstock.¹³

Tar was observed on the filters of the HPFFB collection system (see Figure 2) when Petcoke B was fed, although essentially no tar was observed when feeding Petcoke A. The tar that resulted from Petcoke B likely originated from the Type 2 char particles. The average tar yield of the experimental runs when feeding Petcoke B in the HPFFB reactor was 1.4 wt %, although tar yields as high as 2.3 wt % were measured. Tar is important to consider because any nondepleted tar yields in industrial processes can cause problems by corroding equipment, causing damage to motors and turbines, lowering catalyst efficiency, and condensing in transfer lines.^{31–33}

Gasification Model. Although more complicated models exist,^{13,15,34} the mass release data from the CO₂ gasification petcoke experiments in the HPFFB reactor were modeled with a first-order global model^{12,13,35} where the rate is normalized by external surface area of the particle:

$$\frac{1}{A_p} \cdot \frac{dm_p}{dt} = -k_{\text{rxn}} \cdot P_{\text{CO}_2, \text{surf}} = - \left[A \cdot \exp \left(\frac{-E}{R \cdot T_p} \right) \right] \cdot P_{\text{CO}_2, \text{surf}} \quad (1)$$

where m_p is the particle mass, t is time, A_p is the external surface area of the assumed-spherical particle ($4 \cdot \pi \cdot r^2$), k_{rxn} is the rate constant of CO₂ gasification, $P_{\text{CO}_2, \text{surf}}$ is the partial pressure of CO₂ at the particle surface, A is the apparent pre-exponential factor, E is apparent activation energy, R is the ideal gas

constant, and T_p is the particle temperature. Fitting these data to a more sophisticated model will be performed in the future.

The rate in eq 1 was integrated numerically, and is negative because char loses mass during gasification. The kinetic parameters A and E for the model in eq 1 were determined by minimizing the sum-squared error between predicted and measured gasification mass release data.

Since only the gas temperature (T_{gas}) was measured, T_p was solved using an energy balance on the particle at each time step:

$$m_p \cdot C_p \cdot \frac{dT_p}{dt} = h_c \cdot A_p \cdot (T_{\text{gas}} - T_p) + \epsilon_p \cdot \sigma \cdot A_p \cdot (T_{\text{surr}}^4 - T_p^4) + \frac{dm_p}{dt} \cdot \Delta H_{\text{rxn}} \quad (2)$$

where C_p is the heat capacity of the particle, h_c is the heat transfer coefficient obtained from the Nusselt number (i.e., $h_c = Nu \cdot k_{\text{gas}} / d_p$), ϵ_p is the emissivity of the char particle ($\epsilon_p = 0.8$ with the assumption that it was similar to that of coal char),³⁶ σ is the Stefan–Boltzmann constant ($5.67 \times 10^{-12} \text{ W/cm}^2/\text{K}$), T_{surr} is the temperature of the surroundings (500 K, because heaters were not used in the reactor), and ΔH_{rxn} is the heat of reaction for the CO₂ gasification reaction. The left-hand side of eq 2 was set equal to zero because the steady state was assumed between small time steps near 0.13 ms. The first term on the right-hand side of eq 2 represents the particle heating due to convective heat transfer. The second term in eq 2 is the radiative heat transfer from the particle, which is negative when $T_p > T_{\text{surr}}$. The last term in eq 2 takes into account the heat of reaction from the reacting particle. This last term is negative from the dm_p/dt term; the CO₂–char gasification reaction is endothermic and hence ΔH_{rxn} is positive. Figure 5 shows gas and particle temperature profiles for Petcoke B at the 10 atm 1909 K HPFFB condition with ~40 mol % CO₂ in the postflame environment. The particle temperature profile in the figure was calculated using eq 2.

Although the first-order gasification model in eq 1 lumps any pore diffusion effects into the regressed kinetic parameters, external film mass transfer must be modeled to calculate the partial pressure of reactant gas at the particle surface. The mass transfer through the particle boundary layer is set to equal to the reaction rate at each step:

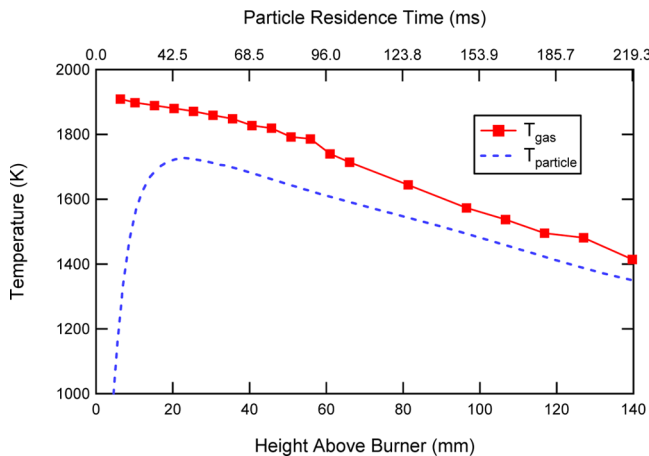


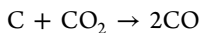
Figure 5. Measured centerline gas temperature profile and calculated Pet coke B particle temperature profile at the 10 atm ~40 mol % CO₂ HPFFB condition.

$$k_{\text{rxn}} P_{\text{CO}_2,\text{surf}} = \nu \cdot h_m \cdot \left(\frac{P_{\text{CO}_2,\infty}}{R \cdot T_{\text{gas}}} - \frac{P_{\text{CO}_2,\text{surf}}}{R \cdot T_p} \right) \quad (3)$$

which can be solved for the partial pressure of CO₂ at the surface as follows:

$$P_{\text{CO}_2,\text{surf}} = \frac{\nu \cdot h_m \cdot P_{\text{CO}_2,\infty}}{R \cdot T_{\text{gas}} \left[k_{\text{rxn}} + \frac{\nu \cdot h_m}{R \cdot T_p} \right]} \quad (4)$$

where ν is the mass of carbon (in grams) that react per mole of reactant, h_m is the mass transfer coefficient taken from the Sherwood number (i.e., $h_m = Sh \cdot D_{\text{AB}} / d_p$), and $P_{\text{CO}_2,\infty}$ is the partial pressure of CO₂ in the bulk gas. In the case of CO₂ gasification, ν was (12 g C/1 mol CO₂) from the following reaction:



The heat of reaction, ΔH_{rxn} , for gasification was calculated using empirical correlations and coefficients from the Gordon–McBride database,³⁷ resulting in an approximate value of 13 700 J/g for CO₂ char gasification reaction (although ΔH_{rxn} is dependent on particle temperature). As other researchers have assumed previously,^{13,38} char was assumed to have properties of graphite in the calculations for ΔH_{rxn} .

The gas thermal conductivity (k_{gas}) was estimated using the k_{gas} values of individual gas species present in the HPFFB postflame environment weighted by their respective mole fractions. The thermal conductivity of individual gas species was estimated using the empirical correlation $k_{\text{gas}}(T) = a \cdot T^b$ with reported values of “ a ” and “ b ”³⁹ evaluated at the film temperature (i.e., average of T_{gas} and T_p).

The binary diffusion coefficients (D_{AB}) required in the mass transfer coefficient (h_m) calculation came from various sources including both published values,⁴⁰ and those fit to an empirical equation based on Chapman–Enskog kinetic theory.³⁹ The diffusion coefficient was evaluated at the film temperature, was inversely proportional to pressure, and directly proportional to temperature raised to a power.

Similar to the reaction conditions in a commercial gasifier, both CO₂ and CO were present in the postflame environment of the HPFFB reactor. The amount of CO present in the four gas conditions used in this study was about 10 mol % (see Table 2), which is important to acknowledge because CO is known to inhibit the CO₂/char gasification reaction. The char conversion kinetics (CCK)^{13,15} coal model was run for 60 μm Illinois #6 coal char at similar reaction conditions⁴¹ as used in this study (see Table 2) to gain insight about the effect of CO on the measured particle mass loss in the HPFFB pet coke gasification experiments. A 5-step gasification kinetic mechanism in the CCK model allowed the effect of CO inhibition to be assessed; the model predicted that the final daf mass release values (char basis) for the coal char were on average 16% lower than when the char gasification occurred at conditions free of CO. The CO inhibition effect may have been of similar magnitude for the pet coke gasification measurements. However, with the limited data available, the first-order modeling for pet coke gasification performed in this study was performed without treating the effect of CO inhibition.

In this study, extents of char gasification were measured at each of the 4 HPFFB gas conditions (see Table 2) using different collection heights above the burner for measurements at low, medium, and high particle residence times. The lowest collection height that served as the initial condition was typically near 25 mm, which was after the initial rise in particle temperature inside the reactor (see Figure 5). Hence, the derived kinetic parameters in this study were not affected by any uncertainties in particle temperature histories between the point of injection and the first collection height.

Table 4. Summary of First-Order Kinetic Parameters and Reaction Conditions for CO₂ Gasification of Petcoke A and B in the HPFFB Reactor

			Pet coke A		Pet coke B	
			$P_{\text{CO}_2,\text{surf}}$ range (atm)		$P_{\text{CO}_2,\text{surf}}$ range (atm)	
P_{total} (atm)	$T_{\text{gas,max}}$ (K)	mol % CO ₂	T_p range (K)		T_p range (K)	
15	1848	~90	1174–1491	9.7–12.2	1201–1595	11.1–12.6
10	1808	~90	1184–1497	7.0–8.2	1209–1630	7.6–8.5
15	1891	~40	1266–1636	4.5–5.5	1293–1699	5.2–5.7
10	1909	~40	1322–1662	3.2–3.7	1349–1718	3.6–3.8

Modeling Results. The optimized kinetic parameters regressed from the data sets of Petcoke A and B are summarized in Table 4. Because the experimental conditions at which char is generated can affect gasification rates,⁴² it is important to note that the reported kinetic parameters in Table 4 were for petcoke that was pyrolyzed *in situ* at high initial particle heating rates and gasified during short reaction times (<300 ms) at elevated pressure. The maximum initial particle heating rates for Petcoke A and B in the gasification experiments were 6.06×10^4 and 7.55×10^4 K/s, respectively. Calculated ranges of T_p and $P_{CO_2,surf}$ for the petcoke data sets are also included in Table 4, as calculated by eqs 2 and 3, respectively. Complete details of the petcoke gasification data are reported elsewhere.¹⁶

It is important when measuring particle kinetics at high temperature to ensure that the measurements are not entirely controlled by film diffusion. The χ -factor^{43,44} provides an indication of the effect of film diffusion on the measured gasification rates, and ranges from 0 and 1. The χ -factor is defined here as the measured gasification rate divided by the maximum rate under film-diffusion control. When the concentration of reactant gas is approximately zero at the particle surface, the rate is entirely controlled by diffusion of reactant gas to the particle surface and the maximum rate occurs. The maximum χ -factor in the petcoke data sets was 0.15, which indicates that the measured rates did not occur in the Zone III regime where film diffusion controls.

Figure 6 shows an example of the fit of the first-order global model to Petcoke B data collected from the HPFFB reactor at

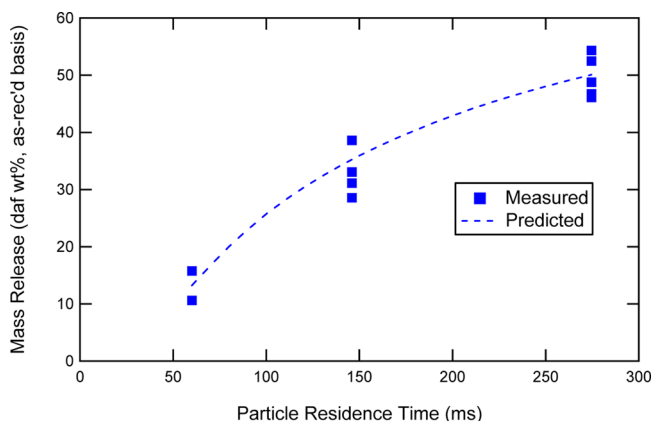


Figure 6. Comparison of measured and modeled mass release of Petcoke B at the 15 atm HPPFB condition where $T_{gas,max} = 1848$ K in an environment with ~90 mol % CO_2 .

the 15 atm condition where the peak gas temperature was 1848 K. The mass release values measured at the lowest residence time serve as the initial condition for the modeling, and the mass release measured at the two higher particle residence times are used to evaluate predicted gasification rates. The parity plots in Figure 7 show how the mass release predicted by the first-order gasification model using kinetic parameters in Table 4 compared with the measured petcoke mass release data (on a char basis). The relative error values reported in Table 4 are an indication of how well the first-order global model predicted the experimental mass release values. The relatively good fit of the model to experimental data is encouraging considering the simplicity of the model.

When the reactivity data of 2 feedstocks have been fit to the same first-order model and they both have the same E value, convenient rate comparisons can be easily performed by using ratios of their A values. For example, the kinetic parameters in Table 4 suggest that Petcoke A is about 2.4 (i.e., $0.1862/0.0771$) times more reactive to CO_2 gasification than Petcoke B when the mass release data were fit to the first-order global model.

Because gasification rates can be a function of conversion, it is important to note that the reported kinetic parameters in Table 4 were for data where Petcoke A and B reached maximum conversions of 55.5 and 41.0 wt % (daf) on a char basis, respectively. It is unclear from the literature how conversion degree affects CO_2 gasification rates of petcoke. Although Gu et al.⁷ measured nearly constant CO_2 gasification rates of petcoke at conversions from about 0.1 to 0.9 at isothermal conditions, Zou et al.⁶ observed a distinct maximum in CO_2 gasification rates near a conversion of 0.3.

The Petcoke A and B char data in this study indicated faster CO_2 gasification rates than a TGA study⁹ where petcoke char was reacted at similar temperature and CO_2 partial pressure. For example, both Petcoke A and B chars attained conversions of at least 10 wt % (daf char basis) between collection heights of 76 mm to 140 mm above the burner during all 4 of the experimental conditions tested (see Table 2). This implies that measurable mass loss was observed in this study due to CO_2 gasification of petcoke char in an average time of ~115 ms at average particle temperatures between 1238 and 1455 K where average $P_{CO_2,surf}$ values were 3.5–12.4 atm at total pressures of 10 and 15 atm. However, no measurable mass loss occurred in such a short time when petcoke char prepared at atmospheric pressure in N_2 using a heating rate of 20 K/min with a 1 h hold time at 1248 K and a 2 h cooling time was gasified in a TGA in undiluted CO_2 at 1248 K at a total pressure of 13.8 atm.⁹ Perhaps this discrepancy can be related to the vastly different pyrolysis conditions of the petcoke chars. However, no significant CO_2 char gasification was measured for either Petcoke A or B at atmospheric pressure in a postflame environment that contained up to 27 mol % CO_2 at conditions where the average particle temperatures were between 952 and 1546 K using particle residence times up to 102 ms, which seems consistent with the low reactivities observed in other studies.^{4–9} Thus, the high reactivities observed in the current study are limited to petcoke chars generated and gasified at high heating rates and pressures.

Comparison of Petcoke and Coal CO_2 Gasification Rates. Several researchers have reported that the CO_2 gasification reactivity of petcoke is lower than that of coal.^{5,7,8} However, it is important to note that reactivity comparisons are a function of many variables including coal rank, conditions at which the chars were pyrolyzed, and the reaction condition used to gasify the solid fuels. Because both petcoke and coal are gasified commercially in entrained-flow reactors where the maximum residence time is on the order of seconds, it would be implied that their reactivities are similar at the high temperature and pressure conditions characteristic of such reactors.

As an aside, it is important in rate comparisons to consider the differences in how rates can be reported. For example, the majority of rates in this study are dm/dt normalized by particle external surface area (A_p) while the rates from many TGA studies are reported as $dX/dt = (1/m_{o,daf})dm/dt$, where X is

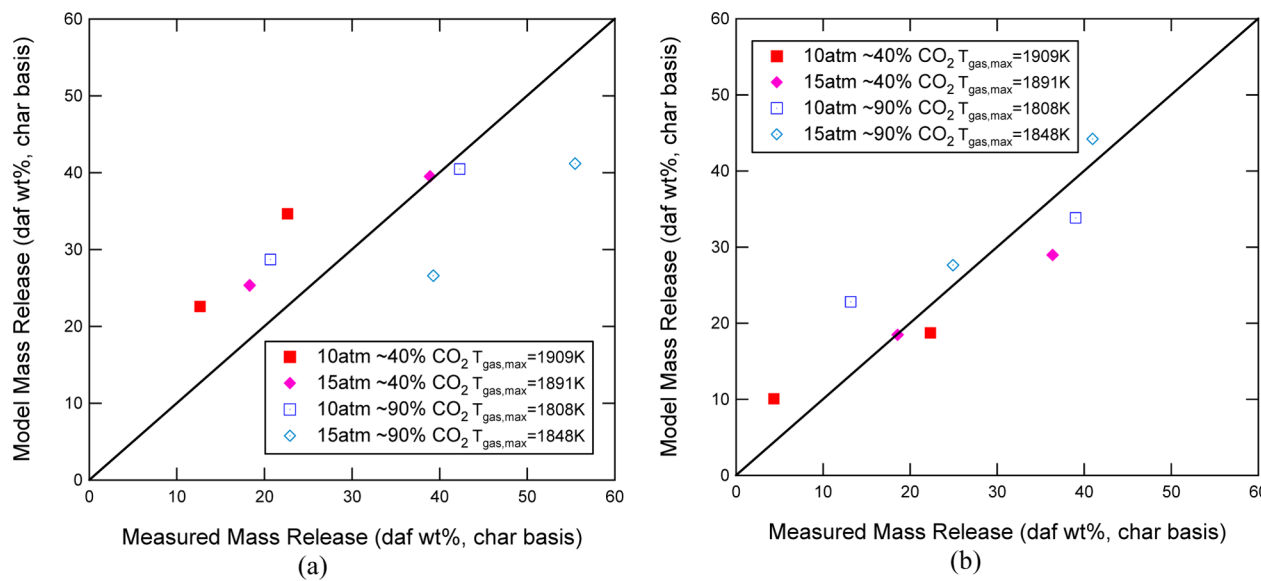


Figure 7. Parity plot of HPFFB gasification mass release data (char basis) for (a) Petcoke A and (b) Petcoke B data.

conversion, t is time, $m_{0,\text{daf}}$ is the starting daf mass of the char sample, and dm/dt is the rate of change in mass.

Wu et al.⁸ reported gasification conversion times for chars of petcoke and Shenhua coal that had been prepared at a heating rate of 6 K/min with 20 min hold times at 950, 1200, and 1400 °C. When these samples were gasified by CO₂ in a TGA at 950 °C at atmospheric pressure, the petcoke char took 14.9, 4.8, and 1.4 times longer to reach 50% conversion than the coal char when comparing chars pyrolyzed at 950, 1200, and 1400 °C, respectively. Thus, it is seen how pyrolysis conditions (pyrolysis temperature, in this case) affected the rate comparisons between petcoke and coal chars. Gu et al.⁷ reported gasification conversion times of both Shenfu coal char that had been pyrolyzed rapidly at 1673 K in a falling reactor and petcoke. The two samples were gasified isothermally by CO₂ at temperatures ranging from 1223 to 1673 K at atmospheric pressure. The reaction times for petcoke to reach 50% conversion were 21.2, 15.6, 7.1, 2.6, 2.3, and 1.9 times longer than those for the coal char at gasification temperatures of 1223, 1273, 1373, 1473, 1573, and 1673 K, respectively. Thus, it appears that any large discrepancy between petcoke and coal CO₂ gasification rates at low temperature is diminished greatly at higher temperatures. However, the researchers did not analyze the effect of external mass transfer resistance at the high temperatures tested, which makes comparisons difficult.

As part of this study, CO₂ gasification rates of Illinois #6 coal char and petcoke were compared at the 15 atm condition of the HPFFB reactor in ~90 mol % CO₂ where the peak centerline gas temperature was 1848 K (see Table 2). Collection heights of 25, 76, and 140 mm were used in the Illinois #6 coal experiments, which corresponded to particle residence times in the range 52–247 ms. It would have been ideal to have the coal pyrolyze in situ followed immediately by CO₂ gasification of the char, as was done when feeding the petcoke samples in the HPFFB reactor. However, soot contamination of the coal char obscured the measured extents of gasification, so a char reinjection technique was implemented, similar to the work of others.^{15,38} It has been reported that capture and reinjection of coal char had little effect on the measured reactivity from data

taken when feeding Illinois #6 coal through an entrained-flow reactor using a single pass or multiple reinjections.³⁸

To generate coal char for CO₂ gasification experiments, raw Illinois #6 coal of the size range 45–75 μm was pyrolyzed at 15 atm total pressure in the HPFFB at a peak gas temperature near 1850 K for ~45 ms utilizing a collection height of 19 mm. A slightly O₂-rich (1.6 mol %) postflame environment was used in order to oxidize the tar before soot could be formed, which allowed the collection of fully pyrolyzed, soot-free coal char. Both the coal pyrolysis and subsequent CO₂ gasification experiments were conducted at 15 atm total pressure. The Illinois #6 coal char used in subsequent gasification experiments was in the size range 75–106 μm (85.3 μm mass mean) because the particles swelled during pyrolysis and this fraction contained the highest yield of particles. Additional properties of the coal char were included in Table 1. Figure 8 shows a SEM image of the pyrolyzed Illinois #6 char that acted as the feedstock material during CO₂ gasification experiments in the HPFFB reactor.

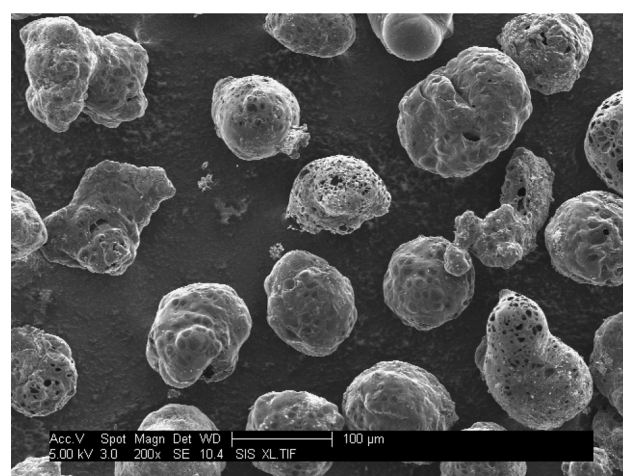


Figure 8. SEM image of 75–106 μm Illinois #6 coal char pyrolyzed at 15 atm in the HPFFB reactor that served as feedstock material for CO₂ gasification experiments.

Figure 9 summarizes measured mass release values on a daf char basis of Petcoke A, Petcoke B, and Illinois #6 coal char

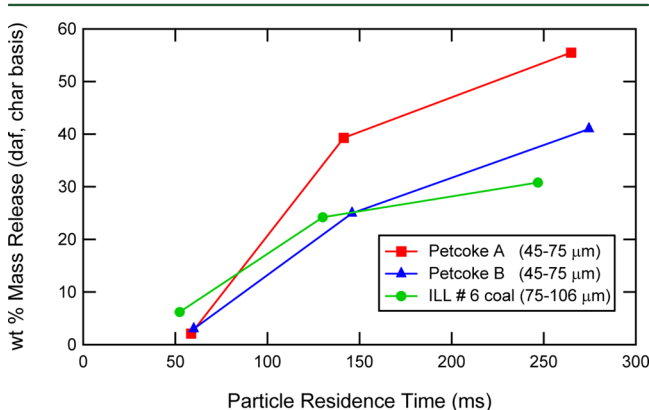


Figure 9. Comparison of mass release (char basis) of Petcoke A, Petcoke B, and ILL #6 coal char at 15 atm $T_{\text{gas},\text{max}} = 1848$ K conditions in the HPFFB in ~90 mol % CO_2 .

after these feedstocks were fed in the HPFFB at 15 atm and $T_{\text{gas},\text{max}} = 1848$ K conditions. The measured mass release values for the coal char in Figure 9 were the average from 2 to 3 experiments, and the replicate mass release values were within on average 2.8 wt % of the previously measured value(s). Petcoke mass release values in Figure 9 were the average of 2–5 experiments, and the replicate mass release values were within on average 4.3 and 4.8 wt % of the previously measured value(s) for Petcoke A and B, respectively. Both petcoke samples gasified to a higher conversion on a char basis when compared to the coal char. However, it is difficult to determine which feedstock had the highest reactivity when compared at the same T_p and $P_{\text{CO}_2,\text{surf}}$ values from simply viewing the figure because each feedstock reacted at particle temperature and $P_{\text{CO}_2,\text{surf}}$ histories that were specific to each feedstock.

To equalize the data in Figure 9 and make a comparison of char CO_2 gasification rate at the same conditions (T_p and $P_{\text{CO}_2,\text{surf}}$), the optimal kinetic parameters for the first-order model were regressed from the ILL #6 coal data and then compared with the petcoke rates using kinetic parameters in Table 4. Regressed values of A and E from the ILL #6 data were 0.6818 g/cm²/s/atm and 121.3 kJ/mol, respectively. For the reactivity comparison, the first-order rate ($(1/A_p) dm/dt$) was converted to dX/dt (or $1/m_{o,\text{daf}} dm/dt$, which is how rates are often compared in other studies) by its multiplication by $(A_p/m_{o,\text{daf}})$, where A_p is the external surface area of a particle ($4\pi r^2$), and $m_{o,\text{daf}}$ is the constant daf mass of a particle after complete pyrolysis. Values of dX/dt at the same condition ($P_{\text{CO}_2,\text{surf}} = 11$ atm and $T_p = 1500$ K) for the three feedstocks are summarized in Figure 10. The CO_2 char gasification reactivities at this condition exhibited the following order: Petcoke A > Petcoke B > Illinois #6 coal. Hence, the reactivity comparison shows that both petcoke had a higher reactivity than the Illinois #6 coal char from entrained-flow experiments conducted at high temperature, pressure, and initial particle heating rates.

The N_2 and CO_2 surface areas of the chars collected from the 15 atm $T_{\text{gas},\text{max}} = 1848$ K ~90 mol % CO_2 condition (see Figure 9) were measured and are summarized in Figure 11a and b, respectively. Calculating dX/dt as was done for Figure 10 using internal surface areas rather than external surface areas yields the same result that both petcoke samples were more reactive

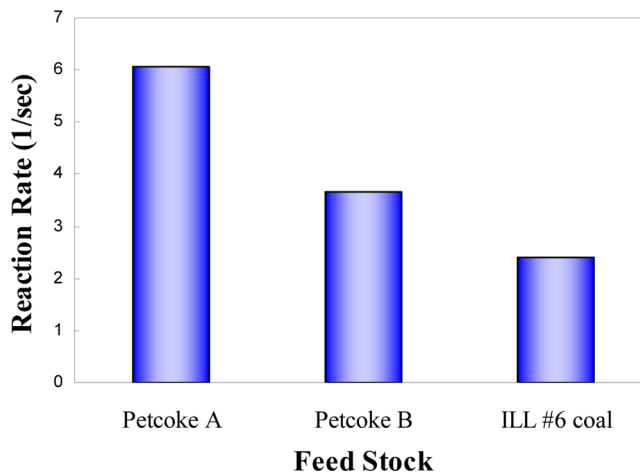


Figure 10. Comparison of the CO_2 gasification rates (dX/dt) of Petcoke A, Petcoke B, and ILL #6 coal char at $P_{\text{CO}_2,\text{surf}} = 11$ atm and $T_p = 1500$ K using kinetic parameters regressed in this study.

than the coal char at the $P_{\text{CO}_2,\text{surf}} = 11$ atm and $T_p = 1500$ K condition, although using internal surface areas in the calculation caused the rate ratio between petcoke and coal char to increase by factors of about 1.5 and 2 for Petcoke A and B, respectively.

4. CONCLUSIONS

The gasification of two petroleum coke samples from industry was studied in this research at conditions of high initial particle heating rate, temperature, and pressure in an entrained-flow reactor. The ASTM volatiles values of both Petcoke A and B were good approximations of the pyrolysis mass release at conditions of atmospheric pressure and high particle heating rate, which differs from other solid fuels such as coal and biomass that typically have increased pyrolysis volatile yields at high heating rate. The morphology of Petcoke A and B chars were evaluated from SEM images of partially gasified samples collected from the HPFFB reactor. The structure of Petcoke A had cracks in its surface, but otherwise appeared very similar to that of its raw feedstock. The cracks did not appear to be significant enough to cause particle fracturing, and are thought to be the result of the volatiles during pyrolysis quickly escaping the particle interior at the experimental conditions of high initial particle heating rate. Petcoke B char contained a small fraction of swollen, thin-shelled particles that resembled pyrolyzed bituminous coal chars from high heating rate conditions. These swollen Petcoke B char particles had little to no pore network internally, and likely did not comprise a high mass fraction of the char due to the very low density of cenospheric particles.

The petcoke CO_2 gasification experiments were conducted at total pressures of 10 and 15 atm in the HPFFB reactor at conditions where the bulk phase consisted of ~40 and ~90 mol % CO_2 using peak centerline gas temperatures up to 1909 K. Mass release caused by CO_2 char gasification was measured for these two petcoke samples (45–75 µm) following in situ pyrolysis in the HPFFB reactor, and was used to regress optimal kinetic parameters using a global first-order model. Over the range of experimental conditions studied, the char CO_2 gasification rate per external surface area ($1/A_p dm/dt$) for Petcoke A char was about 2.4 times higher than that for Petcoke B char. The CO_2 char gasification conversion rates

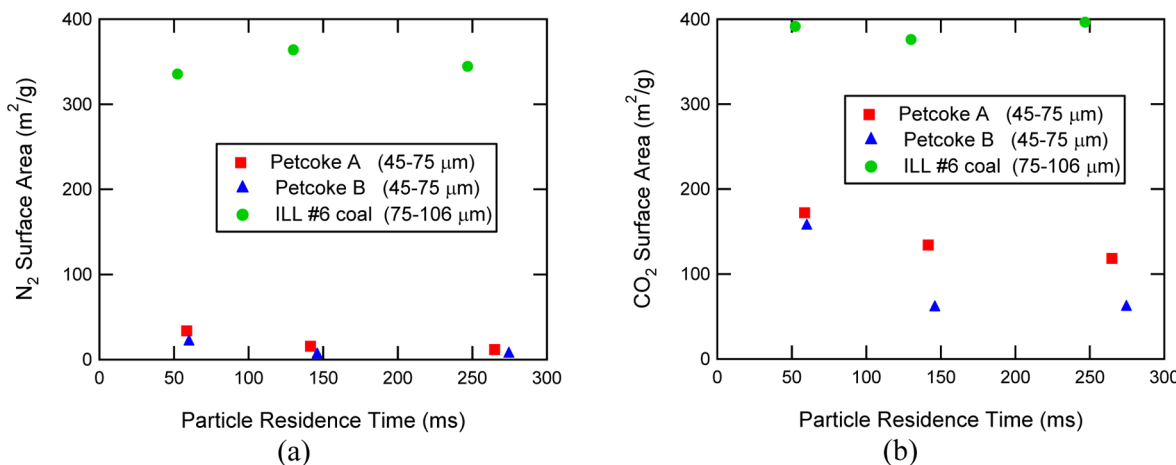


Figure 11. Measured internal surface areas by (a) N_2 and (b) CO_2 of chars used in the petcoke vs ILL #6 coal char comparison and corresponds to data in Figure 9.

(dX/dt) for both Petcoke A and B were shown to be higher than that for Illinois #6 coal at conditions in the HPFF reactor, even though most reactivity comparisons between petcoke and coal at lower temperatures and pressures typically result in coal being more reactive. The reported petcoke char gasification rates in this study are thought to be representative of those from an entrained-flow gasifier because they were measured at similar conditions of elevated temperature and pressure using chars that were pyrolyzed in situ at high heating rates and reacted for short reaction times in entrained flow.

AUTHOR INFORMATION

Corresponding Author

*T. H. Fletcher. Address: Chemical Engineering Department, 350 CB, Brigham Young University, Provo, UT 84602. E-mail: tom_fletcher@byu.edu.

Notes

The authors declare no competing financial interest.

ACKNOWLEDGMENTS

The authors acknowledge BYU's Microscopy lab for their assistance in obtaining the SEM images.

REFERENCES

- (1) Ellis, P. J.; Paul, C. A. Tutorial: Delayed coking fundamentals, *AICHE Spring National Meeting*, Atlanta, GA, March 5–9, 2000.
- (2) Fisher, P. H. Personal communication with principal consultant of Pet Coke Consulting, LLC, located in Greenbrae, CA. A. Lewis, 2014.
- (3) NETL, National Energy Technology Laboratory Gasification Worldwide Database, 2010. <http://www.netl.doe.gov/research/coal/energy-systems/gasification/gasification-plant-databases> (accessed Feb. 25, 2014).
- (4) Tyler, R. J.; Smith, I. W. Reactivity of petroleum coke to carbon dioxide between 1030 and 1180 k. *Fuel* **1975**, *54* (2), 99–104.
- (5) Zamalloa, M.; Ma, D.; Utigard, T. A. Oxidation rates of industrial cokes with CO_2 and air. *ISIJ Int.* **1995**, *35* (5), 458–463.
- (6) Zou, J. H.; Zhou, Z. J.; Wang, F. C.; Zhang, W.; Dai, Z. H.; Liu, H. F.; Yu, Z. H. Modeling reaction kinetics of petroleum coke gasification with CO_2 . *Chem. Eng. Process.* **2007**, *46* (7), 630–636.
- (7) Gu, J.; Wu, S.; Wu, Y.; Gao, J. CO_2 -gasification reactivity of different carbonaceous materials at elevated temperatures. *Energy Sources, Part A* **2009**, *31* (3), 232–243.
- (8) Wu, Y. Q.; Wu, S. Y.; Gu, J.; Gao, J. S. Differences in physical properties and CO_2 gasification reactivity between coal char and petroleum coke. *Process Saf. Environ. Prot.* **2009**, *87* (5), 323–330.
- (9) Malekshahian, M.; Hill, J. M. Kinetic analysis of CO_2 gasification of petroleum coke at high pressures. *Energy Fuels* **2011**, *25* (9), 4043–4048.
- (10) Wall, T. F.; Liu, G. S.; Wu, H. W.; Roberts, D. G.; Benfell, K. E.; Gupta, S.; Lucas, J. A.; Harris, D. J. The effects of pressure on coal reactions during pulverised coal combustion and gasification. *Prog. Energy Combust. Sci.* **2002**, *28* (5), 405–433.
- (11) Cetin, E.; Moghtaderi, B.; Gupta, R.; Wall, T. F. Biomass gasification kinetics: Influences of pressure and char structure. *Combust. Sci. Technol.* **2005**, *177* (4), 765–791.
- (12) Lewis, A. D. Sawdust pyrolysis and petroleum coke CO_2 gasification at high heating rates. Master's Thesis, Brigham Young University, Provo, UT, 2011.
- (13) Shurtz, R. Effects of pressure on the properties of coal char under gasification conditions at high initial heating rates. Ph.D. Dissertation, Brigham Young University, Provo, UT, 2011.
- (14) Shurtz, R. C.; Hogge, J. W.; Fowers, K. C.; Sorensen, G. S.; Fletcher, T. H. Coal swelling model for pressurized high particle heating rate pyrolysis applications. *Energy Fuels* **2012**, *26* (6), 3612–3627.
- (15) Shurtz, R. C.; Fletcher, T. H. Coal char- CO_2 gasification measurements and modeling in a pressurized flat-flame burner. *Energy Fuels* **2013**, *27* (6), 3022–3038.
- (16) Lewis, A. Gasification of biomass, coal, and petroleum coke at high heating rates and elevated pressure. Ph.D. Dissertation, Brigham Young University, Provo, UT, in progress.
- (17) Borrego, A. G.; Alvarez, D. Comparison of chars obtained under oxy-fuel and conventional pulverized coal combustion atmospheres. *Energy Fuels* **2007**, *21* (6), 3171–3179.
- (18) Borrego, A. G.; Garavaglia, L.; Kalkreuth, W. D. Characteristics of high heating rate biomass chars prepared under N_2 and CO_2 atmospheres. *Int. J. Coal Geol.* **2009**, *77* (3–4), 409–415.
- (19) Jamaluddin, A. S.; Truelove, J. S.; Wall, T. F. Devolatilization of bituminous coals at medium to high heating rates. *Combust. Flame* **1986**, *63* (3), 329–337.
- (20) Solomon, P. R.; Fletcher, T. H.; Pugmire, R. J. Progress in coal pyrolysis. *Fuel* **1993**, *72* (5), 587–597.
- (21) Ma, J. Soot formation during coal pyrolysis. Ph.D. Dissertation, Brigham Young University, Provo, UT, 1996.
- (22) Ma, J.; Fletcher, T. H.; Webb, B. W. Conversion of coal tar to soot during coal pyrolysis in a post-flame environment. In *Twenty-Sixth Symposium (International) on Combustion*; The Combustion Institute: Napoli, Italy, 1996; pp 3161–3167.

- (23) Zhang, H. Nitrogen evolution and soot formation during secondary coal pyrolysis. Ph.D. Dissertation, Brigham Young University, Provo, UT, 2001.
- (24) Zhang, H. F.; Fletcher, T. H. Nitrogen transformations during secondary coal pyrolysis. *Energy Fuels* **2001**, *15* (6), 1512–1522.
- (25) Kocaefe, D.; Charette, A.; Castonguay, L. Green coke pyrolysis - investigation of simultaneous changes in gas and solid-phases. *Fuel* **1995**, *74* (6), 791–799.
- (26) Zamalloa, M.; Utigard, T. A. Characterization of industrial coke structures. *ISIJ Int.* **1995**, *35* (5), 449–457.
- (27) Benfell, K. E.; Liu, G. S.; Roberts, D. G.; Harris, D. J.; Lucas, J. A.; Bailey, J. G.; Wall, T. F. Modeling char combustion: The influence of parent coal petrography and pyrolysis pressure on the structure and intrinsic reactivity of its char. *Proc. Combust. Inst.* **2000**, *28*, 2233–2241.
- (28) Wu, H. W.; Bryant, G.; Benfell, K.; Wall, T. An experimental study on the effect of system pressure on char structure of an australian bituminous coal. *Energy Fuels* **2000**, *14* (2), 282–290.
- (29) Milenkova, K. S.; Borrego, A. G.; Alvarez, D.; Xiberta, J.; Menendez, R. Devolatilisation behaviour of petroleum coke under pulverised fuel combustion conditions. *Fuel* **2003**, *82* (15–17), 1883–1891.
- (30) Yu, J. L.; Lucas, J. A.; Wall, T. F. Formation of the structure of chars during devolatilization of pulverized coal and its thermoproperties: A review. *Prog. Energy Combust. Sci.* **2007**, *33* (2), 135–170.
- (31) Baumlin, S.; Broust, F.; Ferrer, M.; Meunier, N.; Marty, E.; Lede, J. The continuous self stirred tank reactor: Measurement of the cracking kinetics of biomass pyrolysis vapours. *Chem. Eng. Sci.* **2005**, *60* (1), 41–55.
- (32) Brage, C.; Yu, Q. H.; Sjostrom, K. Characteristics of evolution of tar from wood pyrolysis in a fixed-bed reactor. *Fuel* **1996**, *75* (2), 213–219.
- (33) Vassilatos, V.; Taralas, G.; Sjostrom, K.; Bjornbom, E. Catalytic cracking of tar in biomass pyrolysis-gas in the presence of calcined dolomite. *Can. J. Chem. Eng.* **1992**, *70* (5), 1008–1013.
- (34) Liu, G. S.; Niksa, S. Coal conversion submodels for design applications at elevated pressures. Part ii. Char gasification. *Prog. Energy Combust. Sci.* **2004**, *30* (6), 679–717.
- (35) Sowa, J. M. Studies of coal nitrogen release chemistry for oxyfuel combustion and chemical additives. M.S. Thesis, Brigham Young University, Provo, UT, 2009.
- (36) Fletcher, T. H. Time-resolved temperature-measurements of individual coal particles during devolatilization. *Combust. Sci. Technol.* **1989**, *63* (1–3), 89–105.
- (37) McBride, B. J.; Zehe, M.; Gordon, S. NASA glenn coefficients for calculating thermodynamic properties of individual species; TP-2002-215556; NASA: Cleveland, OH, 2002.
- (38) Hurt, R.; Sun, J. K.; Lunden, M. A kinetic model of carbon burnout in pulverized coal combustion. *Combust. Flame* **1998**, *113* (1–2), 181–197.
- (39) Mitchell, R. E. A theoretical model of chemically reacting recirculating flow; SAND79-8236; Sandia National Laboratory: Livermore, CA, 1980.
- (40) Incropera, F. P.; Dewitt, D. P. *Fundamentals of heat and mass transfer*, 5th ed.; John Wiley & Sons: Chicago, 2002.
- (41) Lewis, A. Gasification of biomass, coal, and petroleum coke at high heating rates and elevated pressure. Ph.D. Dissertation, Brigham Young University, Provo, UT, in progress.
- (42) Mermoud, F.; Salvador, S.; de Steene, L. V.; Golfier, F. Influence of the pyrolysis heating rate on the steam gasification rate of large wood char particles. *Fuel* **2006**, *85* (10–11), 1473–1482.
- (43) Smith, K. L.; Smoot, L. D.; Fletcher, T. H.; Pugmire, R. J. *The structure and reaction processes of coal*; Plenum Press: New York, 1994.
- (44) Smith, I. W. The combustion rates of coal chars: A review. *Symp. (Int.) Combust., [Proc.]* **1982**, *19* (1), 1045–1065.